

VideoDrafter: Content-Consistent Multi-Scene Video Generation with LLM

Fuchen Long, Zhaofan Qiu, Ting Yao and Tao Mei
HiDream.ai Inc.

{longfc.ustc, zhaofanqiu, tingyao.ustc}@gmail.com
tmei@hidream.ai

<https://videodrafter.github.io>

Abstract

The recent innovations and breakthroughs in diffusion models have significantly expanded the possibilities of generating high-quality videos for the given prompts. Most existing works tackle the single-scene scenario with only one video event occurring in a single background. Extending to generate multi-scene videos nevertheless is not trivial and necessitates to nicely manage the logic in between while preserving the consistent visual appearance of key content across video scenes. In this paper, we propose a novel framework, namely VideoDrafter, for content-consistent multi-scene video generation. Technically, VideoDrafter leverages Large Language Models (LLM) to convert the input prompt into comprehensive multi-scene script that benefits from the logical knowledge learnt by LLM. The script for each scene includes a prompt describing the event, the foreground/background entities, as well as camera movement. VideoDrafter identifies the common entities throughout the script and asks LLM to detail each entity. The resultant entity description is then fed into a text-to-image model to generate a reference image for each entity. Finally, VideoDrafter outputs a multi-scene video by generating each scene video via a diffusion process that takes the reference images, the descriptive prompt of the event and camera movement into account. The diffusion model incorporates the reference images as the condition and alignment to strengthen the content consistency of multi-scene videos. Extensive experiments demonstrate that VideoDrafter outperforms the SOTA video generation models in terms of visual quality, content consistency, and user preference.

1. Introduction

Diffusion Probabilistic Models (DPM) have demonstrated high capability in generating high-quality images [4, 11, 12, 31, 32, 40, 44, 46, 62]. DPM approaches image generation as a multi-step sampling process, involving the use of a denoiser network to progressively transform a Gaussian noise



Figure 1. An illustration of the input prompt and the generated multi-scene videos by using our VideoDrafter.

map into an output image. Compared to 2D images, videos have an additional time dimension, which introduces more challenges when extending DPM to video domain. One typical way is to leverage pre-trained text-to-image models to produce video frames [16, 36, 55] or utilize a 3D denoiser network learnt on video data to generate a sequence of frames in an end-to-end manner [2, 8, 9, 13, 30, 43]. Despite having impressive results in the realm of text-to-video generation, most existing works focus on only single-scene videos, featuring one video event in a single background. The generation of multi-scene videos is still a problem not yet fully explored in the literature.

The difficulty of multi-scene video generation generally

originates from two aspects: 1) how to arrange and establish different events in a logical and realistic way for a multi-scene video? 2) how to guarantee the consistency of common entities, e.g., foreground objects or persons, throughout the video? For instance, given an input prompt of “a young man is making cake,” a multi-scene video is usually to present the step-by-step procedure of making a cake, including measuring out the ingredients, pouring the ingredients into a pan, cooking the cake, etc. This necessitates a comprehensive understanding and refinement of the prompt. As such, we propose to mitigate the first issue through capitalizing on Large Language Models (LLM) to rewrite the input prompt into multi-scene video script. LLM inherently abstracts quantities of text data on the Web about the input prompt to produce the script, which describes and decomposes the video logically into multiple scenes. To alleviate the second issue, we exploit the common entities to generate reference images as the additional condition to produce each scene video. The reference images, as the link across scenes, effectively align the content consistency within a multi-scene video.

To consolidate the idea, we present a new framework dubbed as **VideoDrafter** for content-consistent multi-scene video generation. Technically, VideoDrafter first transforms the input prompt into a thorough multi-scene video script by using LLM. The script for each scene consists of the descriptive prompt of the event in the scene, a list of foreground objects or persons, the background, and camera movement. VideoDrafter then identifies common entities that appear across multiple scenes and requests LLM to enrich each entity. The resultant entity description is fed into a pre-trained Stable Diffusion [40] model to produce a reference image for each entity. Finally, VideoDrafter outputs a multi-scene video via involving two diffusion models, i.e., **VideoDrafter-Img** and **VideoDrafter-Vid**. VideoDrafter-Img is dedicated to incorporating the descriptive prompt of the event and the reference images of entities in each scene as the condition to generate a scene-reference image. VideoDrafter-Vid takes the scene-reference image plus temporal dynamics of the action depicted in the descriptive prompt of the event and camera movement in the script as the inputs and produces a video clip for each scene.

The main contribution of this work is the proposal of VideoDrafter for generating content-consistent multi-scene videos. The solution also leads to the elegant views of how to use LLM to properly arrange the content of multi-scene videos and how to generate visually consistent entities across scenes, which are problems seldom investigated in the literature. Extensive experiments conducted on several public benchmarks demonstrate that VideoDrafter outperforms state-of-the-art video generation models in terms of visual quality, content consistency and user preference.

2. Related Work

Image generation is a fundamental challenge of computer vision and has evolved rapidly in the past decade. Recent advances in Diffusion Probabilistic Models (DPM) have led to remarkable improvements in generating high-fidelity images [2, 4, 11, 12, 28, 29, 31–33, 39, 40, 44–46, 62]. DPM is a category of generative models that utilizes a sequential sampling process to convert random Gaussian noise into high-quality images. For example, GLIDE [33] and DALL-E 2 [39] exploit the sampling process in the pixel space, conditioned on the text prompt using classifier-free guidance [11]. Nevertheless, training a powerful denoising network remains challenging due to high computational cost and memory demand associated with sampling at the pixel level. To mitigate this problem, Latent Diffusion Models (LDM) [40] employ sampling in the latent feature space that is established by a pre-trained autoencoder, leading to the improvements on computation efficiency and image quality. Furthermore, the application of DPM is further enhanced by incorporating advanced sampling strategies [28, 29, 45] and additional control signals [31, 62].

Video generation is a natural extension of image generation in video domain. The early approaches, e.g., ImagenVideo [13] and Make-A-Video [43], train video diffusion models in the pixel space, resulting in high computational complexity. Following LDM in image domain, several works [2, 8, 30] propose to exploit the sampling process in the latent feature space for video generation. These works extend the 2D UNet with transformer layers [20, 57, 58] in LDM to 3D UNet by injecting temporal self-attentions [25, 26] and/or temporal convolutions [24, 27, 38]. For instance, Video LDM [2] and Animatediff [8] focus on training the injected temporal layers while freezing the spatial layers to preserve the ability of the pre-trained image diffusion model. VideoFusion [30] decomposes the 3D noise into a 2D base noise shared across frames and a 3D residual noise, enhancing the correlation between frames. However, the generated videos usually have a limited time duration, typically around 16 frames. Consequently, some recent researches emerge to generate long videos by an extrapolation strategy or hierarchical architecture [9, 21, 48, 49, 60]. In addition, video editing techniques utilize the input video as a condition and generate a video by modifying the style or key object of the input video [6, 7, 9, 15, 35, 36, 42, 50, 53, 55, 59].

In short, our work in this paper focuses on content-consistent multi-scene video generation. The most related work is [22], which aligns the appearance of entities across scenes through the bounding boxes provided by LLM. Ours is different in the way that we explicitly determine the appearance of entities by generating reference images, which serve as a link across scenes and effectively enhance the content consistency within a multi-scene video.

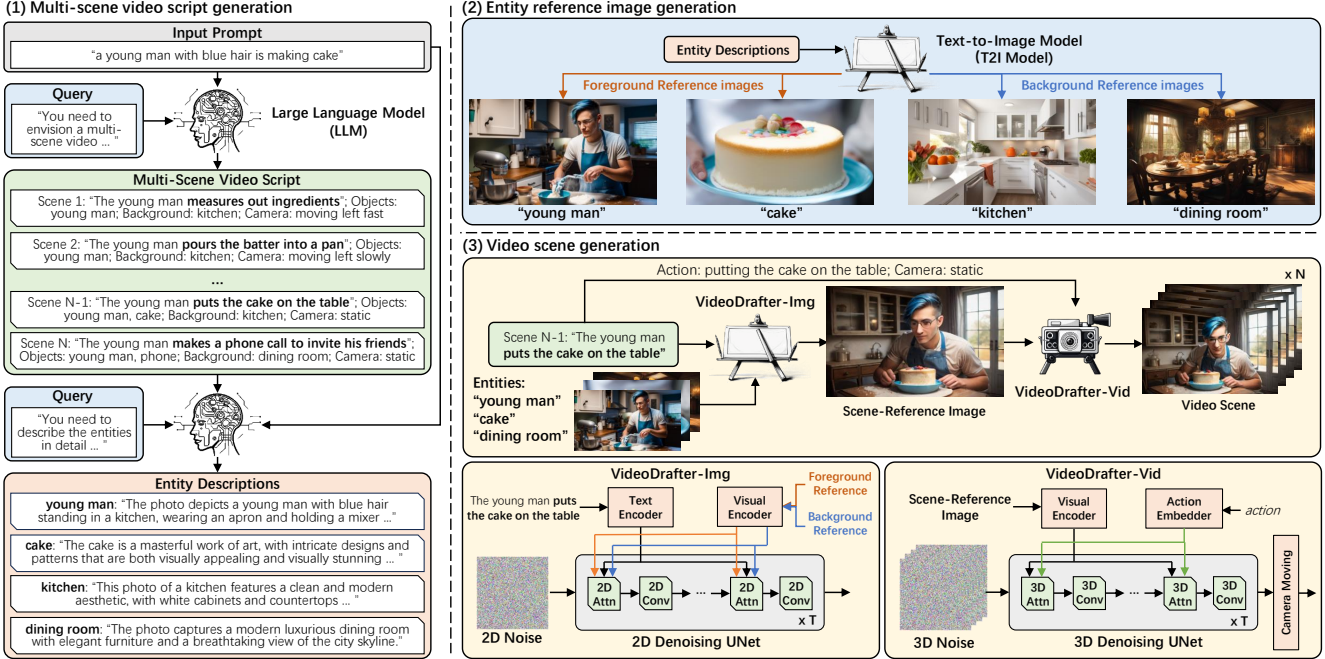


Figure 2. An overview of our VideoDrafter framework for content-consistent multi-scene video generation. VideoDrafter consists of three main stages: (1) multi-scene video script generation, (2) entity reference image generation, and (3) video scene generation. In the first stage, LLM is utilized to convert the input prompt into a comprehensive multi-scene script. The script for each scene includes the descriptive prompt of the event in the scene, a list of foreground objects or persons, the background, and camera movement. We then request LLM to detail the common foreground/background entities across scenes. These entity descriptions are fed into a text-to-image (T2I) model to produce reference images in the second stage. Finally, in the third stage, VideoDrafter-Img exploits the descriptive prompt of the event and the reference images of entities in each scene as the condition to generate a scene-reference image. VideoDrafter-Vid takes the scene-reference image plus temporal dynamics of the action depicted in the descriptive prompt of the event and camera movement in the script as the inputs and produces a video clip for each scene.

3. VideoDrafter

This section presents the proposed VideoDrafter framework for content-consistent multi-scene video generation. Figure 2 illustrates an overview of VideoDrafter framework, consisting of three main stages: (1) multi-scene video script generation (Sec. 3.1), (2) entity reference image generation (Sec. 3.2), and (3) video scene generation (Sec. 3.3).

3.1. Multi-Scene Video Script Generation

As depicted in Figure 2(1), VideoDrafter utilizes LLM to convert the input prompt into a comprehensive multi-scene script. In view of its high deployment flexibility and inference efficiency, we use the open-source ChatGLM3-6B model [5, 61]. The LLM is requested by a pre-defined query, “You need to envision a multi-scene video and describe each scene ...”, to treat the input prompt as the theme, logically decompose the video into multiple scenes and generate a script for each scene in the following format:

$$\begin{aligned}
 & [\text{Scene 1: prompt, foreground, background, camera move}]; \\
 & [\text{Scene 2: prompt, foreground, background, camera move}]; \\
 & \dots \\
 & [\text{Scene } N: \text{prompt, foreground, background, camera move}].
 \end{aligned} \tag{1}$$

Here N denotes the number of video scenes, which is determined by the LLM. For each scene, the descriptive prompt of the event in the scene, a list of foreground objects or persons, the background, and camera movement are provided. The camera movement is restricted to a close-set of directions $\{\text{static, left, right, up, down, forward, backward}\}$ and speeds $\{\text{slow, medium, fast}\}$.

Next, VideoDrafter identifies the common entities, which include foreground objects or persons and background locations. To achieve this, we ask the LLM to assign the common object, person, or background the same name across scenes when generating the video script. Therefore, we strictly match the name of entities and discover the entities that appear in multiple scenes. To further improve the quality of the video script, we employ the capability of the LLM for multi-round dialogue. Specifically, we start the dialogue by asking the LLM to specify the key aspects with respect to the entity, such as “What are the aspects that should be considered when describing a photo of a young man in detail?” In the next round of dialogue, we request the LLM to describe the entity from the viewpoints of the given aspects. Moreover, the original prompt is also taken as the input to the LLM to ensure that the essential charac-

teristics, e.g., “blue hair” of the young man, are emphasized in entity description generation.

Please note that the GPT-4 [34] can also be used for script generation, but it incurs an additional 0.12 USD for the GPT-4 API call per query. In VideoDrafter, we leverage the open-source ChatGLM3-6B and perform the inference on our devices to circumvent the need for API call. Nevertheless, the scale of ChatGLM3-6B is much smaller, resulting in unstable outcomes that may deviate from the specified script format. To alleviate this issue, we have empirically abstracted the following principles to enhance the stability of open-source LLM:

- Before the dialogue starts, we provide comprehensive instructions to the LLM, delineating the additional requirements, specifying the script format, and offering the examples of the expected outputs.
- For each query, we manually select five in-context examples as the historical context for multi-round dialogue. These examples are very carefully designed to ensure a diverse range of scenes, key objects, and background, and serve to emphasize the required script format for LLM.
- After each round of dialogue, we verify the output format. If the results are seemingly inappropriate, we re-run the entire script generation stage. Such strategy is simple to implement and does not require any additional expenses.

We will provide the full version of our instructions, examples, and queries in the supplementary materials.

3.2. Entity Reference Image Generation

In the second stage of VideoDrafter, we unify the visual appearance of common entities by explicitly generating a reference image for each entities. The reference images act as the link to cohere the content across scenes. We achieve this by first feeding the entity description into a pre-trained Stable Diffusion model for text-to-image generation. Then, we employ the U²-Net [37] model for salient object detection, and segment the foreground and background areas in each resultant image. By utilizing the segmentation masks, we can further remove the background pixels from the foreground references and vice versa, in order to prevent the interference between the foreground and background in the reference images.

3.3. Video Scene Generation

VideoDrafter produces a multi-scene video by generating each scene via the diffusion models by taking the reference images, the descriptive prompt of the event and camera movement into account. This stage involves two primary components: the **VideoDrafter-Img**, which utilizes the descriptive prompt of the event and the reference images of entities in each scene as the condition to generate a scene-reference image, and the **VideoDrafter-Vid**, which employs the scene-reference image plus temporal dynam-

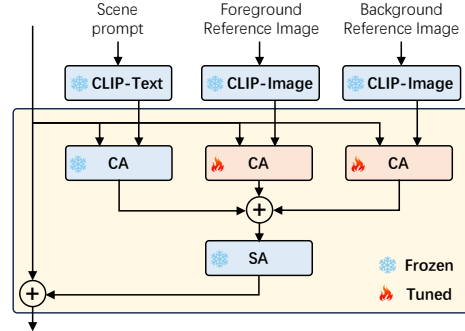


Figure 3. A diagram illustrating the proposed attention module in the VideoDrafter-Img which takes the scene prompt and foreground/background reference images as inputs.

ics of the action depicted in the descriptive prompt of the event and camera movement in the script as the inputs and produces a video clip for each scene.

3.3.1 VideoDrafter-Img

The VideoDrafter-Img component aims to generate a scene-reference image conditioning on the event prompt and entity reference images for each scene. To accomplish this, we remold the Stable Diffusion architecture by replacing the original attention module with a novel attention module that can handle three contexts: the text prompt, foreground reference image, and background reference image. As depicted in Figure 3, we utilize text and visual encoder of a pre-trained CLIP model to extract the sequential text feature $y_t \in \mathbb{R}^{L_t \times C_t}$ and local image features $y_f \in \mathbb{R}^{L_f \times C_f}$ and $y_b \in \mathbb{R}^{L_b \times C_b}$ for the prompt, foreground reference image, and background reference image, respectively. Here, L and C denote the length and the channels of the feature sequence. For the case of multiple foregrounds in one scene, we concatenate the features from all foreground reference images along the length dimension. Given the input feature x , the outputs z of the attention are computed as

$$\begin{aligned} y &= CA_1(x, y_t) + CA_2(x, y_f) + CA_3(x, y_b), \\ z &= x + SA(y), \end{aligned} \quad (2)$$

where CA_1 and SA are the cross-attention and self-attention modules, respectively, in the original Stable Diffusion architecture. We add two additional cross-attention modules, CA_2 and CA_3 , which leverage the guidance provided by entity reference images. Moreover, we propose to optimize the parameters of CA_2 and CA_3 while freezing the other parts of the network.

3.3.2 VideoDrafter-Vid

VideoDrafter-Vid is a video diffusion model that employs the scene-reference image, the action described in the prompt of the event, and camera movement in the script as the inputs. Particularly, we start by extending the Stable

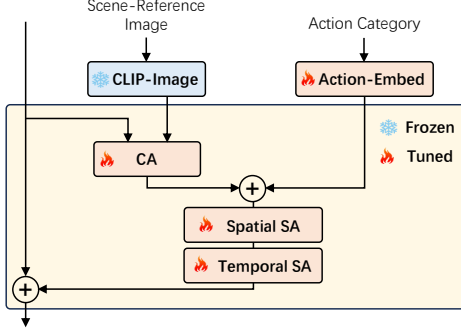


Figure 4. A diagram illustrating the proposed attention module in the VideoDrafter-Vid conditioning on the scene-reference image and the described action category.

Diffusion model to a spatio-temporal form and replacing the original attention module with a new one that is conditioned on the scene-reference image and action category, as shown in Figure 4. Taking 400 action categories in Kinetics [3] as an action vocabulary, an indicator vector $y_a \in [0, 1]^{400}$ is built to infer if each action in the vocabulary exists in the scene prompt and subsequently converted into feature space using a linear embedding f . For the scene-reference image, we use the visual encoder of CLIP to extract the image feature $y_s \in \mathbb{R}^{L_s \times C_s}$, which is then fed into the cross-attention operation. The original self-attention is decomposed into a spatial self-attention (Spatial SA) and a temporal self-attention (Temporal SA), which operate self-attention solely on spatial and temporal dimension, respectively, to reduce computations. Hence, given the input feature x , the attention module is formulated as

$$\begin{aligned} y &= \text{CA}(x, y_s) + f(y_a), \\ z &= x + \text{Temporal SA}(\text{Spatial SA}(y)). \end{aligned} \quad (3)$$

Moreover, we further inject several temporal convolutions behind each spatial convolution into the Stable Diffusion model, to better capture temporal dependencies.

To reflect the camera movement stated by the script in the generated video, we uniquely modify the frames in the intermediate step of sampling process by warping the neighboring frames based on the camera moving direction and speed. We execute this adjustment after the first T_m DDIM sampling steps, followed by continuing the sampling process. Such modification ensures that the resultant video clip maintains the same camera movement as we warp the intermediate frames. In general, setting a small T_m for early modification may not effectively control the camera movement, while a late modification may affect the visual quality of the output videos. In practice, we observe that $T_m=5$ provides a good trade-off. We will detail the formulation of the modification process and the ablation study of the step T_m in our supplementary materials.

4. Experiments

4.1. Datasets

Our VideoDrafter framework is trained on three large-scale datasets: LAION-2B [41], WebVid-10M [1] and HD-VG-130M [52]. The LAION-5B is one of the largest text-image dataset consisting of around 5 billion text-image pairs. To train VideoDrafter-Img, We utilize a subset, namely **LAION-2B**, which focuses on the text prompts in English. The **WebVid-10M** and **HD-VG-130M** are the large-scale single-scene video datasets, containing approximately 10M and 130M text-video pairs, respectively. VideoDrafter-Vid is trained on the combination of WebVid-10M and a randomly chosen 20M subset from HD-VG-130M.

To evaluate video generation, we select the text prompts from three video datasets, i.e., MSR-VTT [56], ActivityNet Captions [18] and Coref-SV [22]. The first one provides the single-scene prompts, while the remaining two datasets comprise multi-scene prompts. The **MSR-VTT** [56] consists of 10K web video clips, each annotated with approximate 20 natural sentences. We utilize the text annotation of validation videos to serve as single-scene prompts in our evaluation. The **ActivityNet Captions** dataset is a multi-event video dataset designed for dense-captioning tasks. Following [22], we randomly sample 165 videos from the validation set and exploit the event captions as the multi-scene prompts. The **Coref-SV** is a multi-scene description dataset, which was constructed by replacing the subject of multi-scene paragraphs in Pororo-SV dataset [17, 19]. Coref-SV samples 10 episodes from the Pororo-SV dataset and replaces the subject with 10 real-world entities, resulting in 100 multi-scene prompts.

4.2. Evaluation Metrics

For the video generation task, we adopt five evaluation metrics. To assess the visual quality of the generated videos, we utilize the average of the per-frame Fréchet Inception Distance (**FID**) [10] and the clip-level Fréchet Video Distance (**FVD**) [47], both of which are commonly used metrics. We also employ the **CLIPSIM** [54] metric to evaluate the alignment between the generated frames and the input prompt. To verify the content consistency, we calculate frame consistency (**Frame Consis.**) by determining the CLIP-similarity between consecutive frames, serving as an intra-scene consistency measure. Additionally, we employ the Grounding-DINO detector [23] to detect common objects across scenes and then calculate the CLIP-similarity between the common objects appeared in different scenes, achieving cross-scene consistency (**Scene Consis.**).

4.3. Implementation Details

We implement our VideoDrafter using the Diffusers codebase on the PyTorch platform.

Table 1. Performance comparisons of VideoDrafter-Img variants with different input references on MSR-VTT validation set.

Input References		FG-SIM	BG-SIM	CLIPSIM
FG Ref.	BG Ref.			
w/o Ref.		0.5162	0.4131	<u>0.3001</u>
✓		0.7919	0.4393	0.2982
	✓	0.5362	<u>0.5742</u>	<u>0.3002</u>
✓	✓	0.8102	0.5861	0.3023

Training stage of VideoDrafter-Img. VideoDrafter-Img is originated from the Stable Diffusion v2.1 model by incorporating two additional cross-attention modules. These modules are initialized from scratch and trained on the text-image pairs from LAION-2B dataset, while other parts of the network are frozen. For each image, we randomly sample a 512×512 patch cropped from the original image, and utilize the U²-Net model to segment the foreground area of each patch. The isolated foreground and background areas serve as the foreground and background reference images, respectively, for guiding the generation of the input patch. We set each minibatch as 512 patches that are processed on 64 A100 GPUs in parallel. The parameters of the model are optimized by AdamW optimizer with a fixed learning rate of 1×10^{-4} for 20K iterations.

Training stage of VideoDrafter-Vid. VideoDrafter-Vid model is developed based on the Stable Diffusion XL framework by inserting temporal attentions and temporal convolutions. The training is carried out on the WebVid-10M and HD-VG-130M datasets. For each video, we randomly sample a 16-frame clip with the resolution of 320×512 and an FPS of 8. The middle frame of the clip is utilized as the scene-reference image. Each minibatch consists of 128 video clips implemented on 64 A100 GPUs in parallel. We utilize the AdamW optimizer with a fixed learning rate of 3×10^{-6} for 480K iterations.

4.4. Experimental Analysis of VideoDrafter

Evaluation on VideoDrafter-Img. We first verify the effectiveness of VideoDrafter-Img in aligning with the input entity reference images. To this end, we take the prompts from MSR-VTT validation set. The input foreground and background reference images are produced by using LLM and Stable Diffusion model. We validate the generated images on the measure of foreground similarity (**FG-SIM**) and background similarity (**BG-SIM**), which are the CLIP-similarity values with the foreground and background reference images, respectively. Table 1 lists the performance comparisons of different VideoDrafter variants by leveraging different input references. Overall, the use of foreground/background reference image as guidance leads to higher FG-SIM/BG-SIM values. The combination of both reference images achieves the highest FG-SIM of 0.8102 and BG-SIM of 0.5861. It is worth noting that all vari-

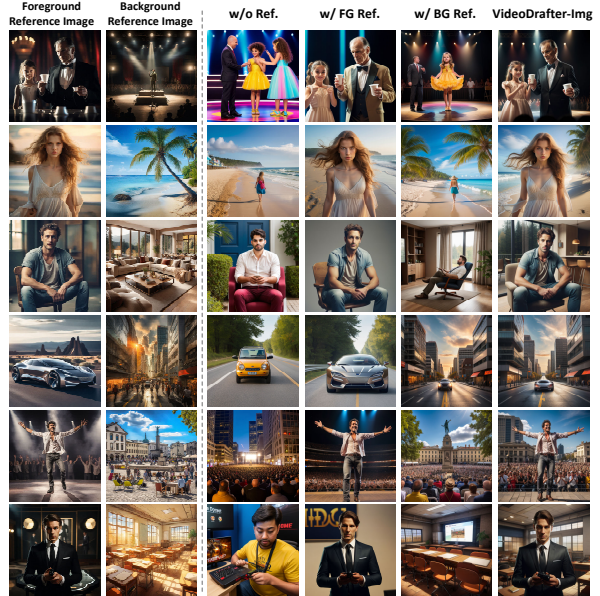


Figure 5. The examples of the foreground and background reference images and the generated scene-reference image by the VideoDrafter-Img variants.

Table 2. Performance comparisons for single-scene video generation with real frame as scene-reference image on WebVid-10M.

Approach	FVD (↓)	Frame Consis. (↑)
RF+VideoComposer [53]	231.0	95.9
RF+VideoDrafter-Vid ⁻	157.3	98.5
RF+VideoDrafter-Vid	116.5	98.8

ants obtain close CLIPSIM values, indicating that the involvement of reference images does not affect the alignment with the input prompts. Figure 5 showcases six generated images by different VideoDrafter-Img variants with various reference images. The results demonstrate the advantage of VideoDrafter-Img to align with the entity reference images.

Evaluation on VideoDrafter-Vid. Next, we assess the visual quality of the single-scene videos generated by VideoDrafter-Vid. We exploit the real frame from the WebVid-10M validation set as the scene-reference image irrespective of the generation quality, and produce a video using the corresponding text prompt, which is referred to as **RF+VideoDrafter-Vid**. We compare our proposal with two baseline models of **RF+VideoComposer** and **RF+VideoDrafter-Vid⁻**. The former employs a pre-trained image animation model by VideoComposer [53] to convert the real frame into a video clip. The latter disables the action guidance in VideoDrafter-Vid. Table 2 presents the performance comparisons for single-scene video generation on the WebVid-10M dataset. With the same scene-reference images, VideoDrafter-Vid⁻ outperforms VideoComposer relatively by 31.9% FVD and 2.7% frame consistency. This improvement is attributed to the deep network architecture and large-scale training set. The performance



Figure 6. Examples of generated multi-scene videos by ModelScopeT2V [51], VideoDirectorGPT [22] and our VideoDrafter utilizing a multi-scene prompt from the Coref-SV dataset. For each video, only the first four scenes are given. The results of VideoDirectorGPT are provided in the project webpage and thus with bounding box annotation.

Table 3. Performance comparisons for single-scene video generation on MSR-VTT validation set. RF indicates whether to utilize the real frame as the reference.

Approach	RF	FID (↓)	FVD (↓)
CogVideo [14]		23.6	-
MagicVideo [63]		-	998
Make-A-Video [43]		13.2	-
VideoComposer [53]		-	580
VideoDirectorGPT [22]		12.2	<u>550</u>
ModelScopeT2V [51]		11.1	<u>550</u>
SD+VideoDrafter-Vid		<u>11.9</u>	381
RF+VideoComposer [53]	✓	31.3	208
RF+VideoDrafter-Vid	✓	10.8	133

is further enhanced to 116.5 FVD and 98.8 frame consistency by RF+VideoDrafter-Vid, verifying the superiority of involving action category guidance to improve visual quality and intra-scene consistency.

Similar performance trends are observed on MSR-VTT dataset, as summarized in Table 3. The methods in this table are grouped into two categories: the methods with or without real frame (RF) as reference. To compare with the generation models without RF, we develop a two-step solution that first generates the scene-reference image by Stable Diffusion, and then converts the image into a video clip by VideoDrafter-Vid, which is denoted as **SD+VideoDrafter-Vid**. Specifically, VideoDrafter-Vid attains the best FVD on both settings with and without a real frame as reference. SD+VideoDrafter-Vid is slightly inferior to ModelScopeT2V in FID. We speculate that this may be the result of not optimizing Stable Diffusion on video frames, resulting in poorer frame quality against ModelScopeT2V. Nevertheless, SD+VideoDrafter-Vid apparently surpasses ModelScopeT2V in FVD, validating the video-level quality by VideoDrafter-Vid.

Table 4. Performance comparisons for multi-scene video generation on ActivityNet Caption dataset.

Approach	FID (↓)	FVD (↓)	Scene Consis. (↑)
ModelScopeT2V [51]	18.1	980	46.0
VideoDirectorGPT [22]	16.5	805	64.8
VideoDrafter w/o Ref.	17.3	624	50.8
VideoDrafter	13.2	395	75.1

Table 5. Performance comparisons for multi-scene video generation on Coref-SV dataset.

Approach	CLIPSIM (↑)	Scene Consis. (↑)
ModelScopeT2V [51]	0.3021	37.9
VideoDirectorGPT [22]	-	42.8
VideoDrafter w/o Ref.	0.3103	40.9
VideoDrafter	0.3304	77.3

4.5. Evaluations on Multi-Scene Video Generation

We validate VideoDrafter for multi-scene video generation on ActivityNet Captions and Coref-SV datasets. Both of the datasets consist of multi-scene prompts, which necessitate the LLM to write the video script based on the given prompt of each scene. We compare with three approaches: ModelScopeT2V, VideoDirectorGPT and VideoDrafter w/o Ref. by disabling the reference images in VideoDrafter. Table 4 details the performance comparisons on ActivityNet Captions. As indicated by the results in the table, VideoDrafter exhibits superior visual quality and better cross-scene consistency. Specifically, VideoDrafter surpasses VideoDrafter w/o Ref. by 24.3 scene consistency, which essentially verifies the effectiveness of incorporating entity reference images. Moreover, VideoDrafter leads to 10.3 and 29.1 improvements in scene consistency over VideoDirectorGPT and ModelScopeT2V, respectively. Similar results are also observed on Coref-SV dataset, as summarized in Table 5. Note that as Coref-SV only offers prompts without the corresponding videos, FID and FVD cannot be mea-

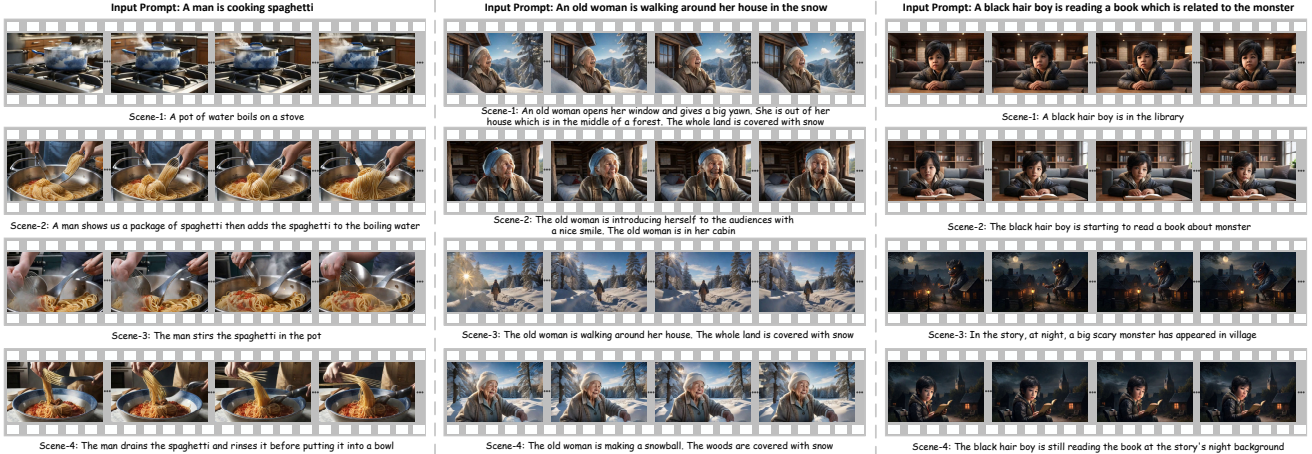


Figure 7. Examples of generated multi-scene videos by VideoDrafter on MSR-VTT. For each video, only the first four scenes are given.

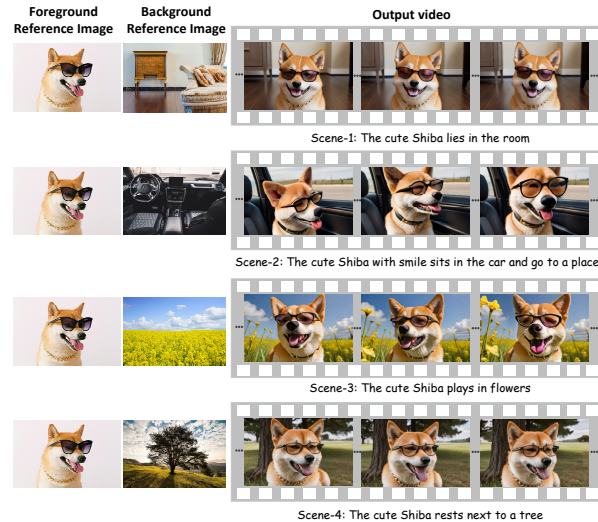


Figure 8. One example of generated multi-scene videos by our VideoDrafter using the real images as entity reference images.

sured for this case. As shown in the table, VideoDrafter again achieves the highest cross-scene consistency of 77.3, making an absolute improvement of 39.4 and 34.5 over ModelScopeT2V and VideoDirectorGPT. Figure 6 shows an example of generated four-scene videos by different approaches on Coref-SV, manifesting the ability of VideoDrafter on generating visually similar entities (e.g., mouse/garden) across scenes. Figure 8 further shows an example of multi-scene video generation by VideoDrafter **using the real images as entity reference images**, which demonstrates the potential of VideoDrafter in customizing the generated objects or environments.

4.6. Human Evaluation

In this section, we conduct a human study to evaluate the entire process of generating multi-scene video from a single prompt. We compare our VideoDrafter with four approaches: **ModelScopeT2V w/o LLM** and **VideoDrafter w/o Ref. w/o LLM** to generate five scenes by duplicating

Table 6. The user study on three criteria: visual quality (VQ), logical coherence (LC) and content consistency (CC).

Approach	VQ (↓)	LC (↓)	CC (↓)
ModelScopeT2V w/o LLM	4.5	4.7	3.9
ModelScopeT2V w/ LLM	4.5	3.8	4.2
VideoDrafter w/o Ref. w/o LLM	2.0	3.0	2.3
VideoDrafter w/o Ref.	2.4	2.3	3.4
VideoDrafter	1.6	1.2	1.2

the input prompt, **ModelScopeT2V w/ LLM** and **VideoDrafter w/o Ref.** to utilize LLM to provide video script as described in Sec. 3.1 while generate each scene individually. We invite 12 evaluators and randomly select 100 prompts from MSR-VTT validation set for human evaluation. We show all the evaluators the five videos generated by each approach plus the given prompt and ask them to rank the five videos from 1 to 5 (good to bad) with respect to the three criteria: visual quality (VQ), logical coherence (LC) and content consistency (CC). For each approach, we average the ranking on each criterion of all the generated videos. As indicated by the results in Table 6, the study proves the impact of LLM generated video script and entity reference images to improve logical coherence and content consistency, respectively. Figure 7 illustrates the examples of the generated multi-scene videos by our VideoDrafter.

5. Conclusions

We have presented a new VideoDrafter framework for content-consistent multi-scene video generation. VideoDrafter involves LLM to benefit from the logical knowledge learnt behind and rewrite the input prompt into a multi-scene video script. Then, VideoDrafter identifies common entities throughout the script and generates a reference image for each entity, which serves as the link across scenes to ensure the appearance consistency. To produce a multi-scene video, VideoDrafter devises two diffusion models of VideoDrafter-Img and VideoDrafter-Vid. VideoDrafter-

Img creates a scene-reference image for each scene based on the corresponding event prompt and entity reference images. VideoDrafter-Vid converts the scene-reference image into a video clip conditioning on the specific action and camera movement. Extensive evaluations on four video benchmarks demonstrate the superior visual quality and content consistency by VideoDrafter over SOTA models.

References

- [1] Max Bain, Arsha Nagrani, Gül Varol, and Andrew Zisserman. Frozen in Time: A Joint Video and Image Encoder for End-to-End Retrieval. In *ICCV*, 2021. 5
- [2] Andreas Blattmann, Robin Rombach, Huan Ling, Tim Dockhorn, Seung Wook Kim, Sanja Fidler, and Karsten Kreis. Align your Latents: High-Resolution Video Synthesis with Latent Diffusion Models. In *CVPR*, 2023. 1, 2
- [3] João Carreira and Andrew Zisserman. Quo Vadis, Action Recognition? A New Model and The Kinetics Dataset. In *CVPR*, 2017. 5
- [4] Prafulla Dhariwal and Alex Nichol. Diffusion Models Beat GANs on Image Synthesis. In *NeurIPS*, 2021. 1, 2
- [5] Zhengxiao Du, Yujie Qian, Xiao Liu, Ming Ding, Jiezhong Qiu, Zhilin Yang, and Jie Tang. GLM: General Language Model Pretraining with Autoregressive Blank Infilling. In *ACL*, 2022. 3
- [6] Patrick Esser, Johnathan Chiu, Parmida Atighehchian, Jonathan Granskog, and Anastasis Germanidis. Structure and Content-guided Video Synthesis with Diffusion Models. In *ICCV*, 2023. 2
- [7] Michal Geyer, Omer Bar-Tal, Shai Bagon, and Tali Dekel. TokenFlow: Consistent Diffusion Features for Consistent Video Editing. *arXiv preprint arXiv:2307.10373*, 2023. 2
- [8] Yuwei Guo, Ceyuan Yang, Anyi Rao, Yaohui Wang, Yu Qiao, Dahua Lin, and Bo Dai. AnimateDiff: Animate Your Personalized Text-to-Image Diffusion Models without Specific Tuning. *arXiv preprint arXiv:2307.04725*, 2023. 1, 2
- [9] Yingqing He, Tianyu Yang, Yong Zhang, Ying Shan, and Qifeng Chen. Latent Video Diffusion Models for High-Fidelity Long Video Generation. *arXiv preprint arXiv:2211.13221*, 2022. 1, 2
- [10] Martin Heusel, Hubert Ramsauer, Thomas Unterthiner, Bernhard Nessler, and Sepp Hochreiter. Gans Trained by a Two Time-Scale Update Rule Converge to a Local Nash Equilibrium. In *NIPS*, 2017. 5
- [11] Jonathan Ho and Tim Salimans. Classifier-Free Diffusion Guidance. *arXiv preprint arXiv:2207.12598*, 2022. 1, 2
- [12] Jonathan Ho, Ajay Jain, and Pieter Abbeel. Denoising Diffusion Probabilistic Models. In *NeurIPS*, 2020. 1, 2
- [13] Jonathan Ho, William Chan, Chitwan Saharia, Jay Whang, Ruiqi Gao, Alexey Gritsenko, Diederik P. Kingma, Ben Poole, Mohammad Norouzi, David J. Fleet, and Tim Salimans. Imagen Video: High Definition Video Generation with Diffusion Models. *arXiv preprint arXiv:2210.02303*, 2022. 1, 2
- [14] Wenyi Hong, Ming Ding, Wendi Zheng, Xinghan Liu, and Jie Tang. CogVideo: Large-Scale Pretraining for Text-to-Video Generation via Transformers. In *ICLR*, 2023. 7
- [15] Zhihao Hu and Dong Xu. VideoControlNet: A Motion-Guided Video-to-Video Translation Framework by Using Diffusion Model with ControlNet. *arXiv preprint arXiv:2307.14073*, 2023. 2
- [16] Levon Khachatryan, Andranik Movsisyan, Vahram Tadevosyan, Roberto Henschel, Zhangyang Wang, Shant Navasardyan, and Humphrey Shi. Text2Video-Zero: Text-to-Image Diffusion Models are Zero-Shot Video Generators. In *ICCV*, 2023. 1
- [17] Kyung-Min Kim, Min-Oh Heo, Seong-Ho Choi, and Byoung-Tak Zhang. DeepStory: Video Story QA by Deep Embedded Memory Networks. In *IJCAI*, 2017. 5
- [18] Ranjay Krishna, Kenji Hata, Frederic Ren, Li Fei-Fei, and Juan Carlos Niebles. Dense-Captioning Events in Videos. In *ICCV*, 2017. 5
- [19] Yitong Li, Zhe Gan, Yelong Shen, Jingjing Liu, Yu Cheng, Yuexin Wu, Lawrence Carin, David Carlson, and Jianfeng Gao. StoryGAN: A Sequential Conditional GAN for Story Visualization. In *CVPR*, 2019. 5
- [20] Yehao Li, Ting Yao, Yingwei Pan, and Tao Mei. Contextual Transformer Networks for Visual Recognition. *IEEE Trans. on PAMI*, 2022. 2
- [21] Jian Liang, Chenfei Wu, Xiaowei Hu, Zhe Gan, Jianfeng Wang, Lijuan Wang, Zicheng Liu, Yuejian Fang, and Nan Duan. NUWA-Infinity: Autoregressive over Autoregressive Generation for Infinite Visual Synthesis. In *NeurIPS*, 2022. 2
- [22] Han Lin, Abhay Zala, Jaemin Cho, and Mohit Bansal. VideoDirectorGPT: Consistent Multi-Scene Video Generation via LLM-Guided Planning. *arXiv preprint arXiv:2309.15091*, 2023. 2, 5, 7
- [23] Shilong Liu, Zhaoyang Zeng, Tianhe Ren, Feng Li, Hao Zhang, Jie Yang, Chunyuan Li, Jianwei Yang, Hang Su, Jun Zhu, et al. Grounding DINO: Marrying Dino with Grounded Pre-Training for Open-Set Object Detection. *arXiv preprint arXiv:2303.05499*, 2023. 5
- [24] Fuchen Long, Ting Yao, Zhaofan Qiu, Xinmei Tian, Jiebo Luo, and Tao Mei. Gaussian Temporal Awareness Networks for Action Localization. In *CVPR*, 2019. 2
- [25] Fuchen Long, Zhaofan Qiu, Yingwei Pan, Ting Yao, Jiebo Luo, and Tao Mei. Stand-Alone Inter-Frame Attention in Video Models. In *CVPR*, 2022. 2
- [26] Fuchen Long, Zhaofan Qiu, Yingwei Pan, Ting Yao, Chongwah Ngo, and Tao Mei. Dynamic Temporal Filtering in Video Models. In *ECCV*, 2022. 2
- [27] Fuchen Long, Ting Yao, Zhaofan Qiu, Xinmei Tian, Jiebo Luo, and Tao Mei. Bi-calibration Networks for Weakly-Supervised Video Representation Learning. *IJCV*, 2023. 2
- [28] Cheng Lu, Yuhao Zhou, Fan Bao, Jianfei Chen, Chongxuan Li, and Jun Zhu. DPM-Solver: A Fast ODE Solver for Diffusion Probabilistic Model Sampling in Around 10 Steps. In *NeurIPS*, 2022. 2
- [29] Cheng Lu, Yuhao Zhou, Fan Bao, Jianfei Chen, Chongxuan Li, and Jun Zhu. DPM-Solver++: Fast Solver for Guided Sampling of Diffusion Probabilistic Models. *arXiv preprint arXiv:2211.01095*, 2023. 2

- [30] Zhengxiong Luo, Dayou Chen, Yingya Zhang, Yan Huang, Liang Wang, Yujun Shen, Deli Zhao, Jingren Zhou, and Tieniu Tan. VideoFusion: Decomposed Diffusion Models for High-Quality Video Generation. In *CVPR*, 2023. 1, 2
- [31] Chong Mou, Xintao Wang, Liangbin Xie, Yanze Wu, Jian Zhang, Zhongang Qi, Ying Shan, and Xiaohu Qie. T2I-Adapter: Learning Adapters to Dig out More Controllable Ability for Text-to-Image Diffusion Models. *arXiv preprint arXiv:2302.08453*, 2023. 1, 2
- [32] Alex Nichol and Prafulla Dhariwal. Improved Denoising Diffusion Probabilistic Models. In *ICML*, 2021. 1
- [33] Alex Nichol, Prafulla Dhariwal, Aditya Ramesh, Pranav Shyam, Pamela Mishkin, Bob McGrew, Ilya Sutskever, and Mark Chen. GLIDE: Towards Photorealistic Image Generation and Editing with Text-Guided Diffusion Models. In *ICML*, 2022. 2
- [34] OpenAI. GPT-4 Technical Report, 2023. 4
- [35] Hao Ouyang, Qiuyu Wang, Yuxi Xiao, Qingyan Bai, Juntao Zhang, Kecheng Zheng, Xiaowei Zhou, Qifeng Chen, and Yujun Shen. CoDeF: Content Deformation Fields for Temporally Consistent Video Processing. *arXiv preprint arXiv:2308.07926*, 2023. 2
- [36] Chenyang Qi, Xiaodong Cun, Yong Zhang, Chenyang Lei, Xintao Wang, Ying Shan, and Qifeng Chen. FateZero: Fusing Attentions for Zero-shot Text-based Video Editing. In *ICCV*, 2023. 1, 2
- [37] Xuebin Qin, Zichen Zhang, Chenyang Huang, Masood Dehghan, Osmar Zaiane, and Martin Jagersand. U2-Net: Going Deeper with Nested U-Structure for Salient Object Detection. *Pattern Recognition*, 2020. 4
- [38] Zhaofan Qiu, Ting Yao, and Tao Mei. Learning Spatio-Temporal Representation with Pseudo-3D Residual Networks. In *ICCV*, 2017. 2
- [39] Aditya Ramesh, Prafulla Dhariwal, Alex Nichol, Casey Chu, and Mark Chen. Hierarchical Text-Conditional Image Generation with CLIP Latents. *arXiv preprint arXiv:2204.06125*, 2022. 2
- [40] Robin Rombach, Andreas Blattmann, Dominik Lorenz, Patrick Esser, and Björn Ommer. High-Resolution Image Synthesis with Latent Diffusion Models. In *CVPR*, 2022. 1, 2
- [41] Christoph Schuhmann, Romain Beaumont, Richard Vencu, Cade Gordon, Ross Wightman, Mehdi Cherti, Theo Coombes, Aarush Katta, Clayton Mullis, Mitchell Wortsman, et al. Laion-5B: An Open Large-Scale Dataset for Training Next Generation Image-Text Models. In *NeurIPS*, 2022. 5
- [42] Chaehun Shin, Heeseung Kim, Che Hyun Lee, Sang gil Lee, and Sungroh Yoon. Edit-A-Video: Single Video Editing with Object-Aware Consistency. *arXiv preprint arXiv:2303.07945*, 2023. 2
- [43] Uriel Singer, Adam Polyak, Thomas Hayes, Xi Yin, Jie An, Songyang Zhang, Qiyuan Hu, Harry Yang, Oron Ashual, Oran Gafni, Devi Parikh, Sonal Gupta, and Yaniv Taigman. Make-a-video: Text-to-Video Generation without Text-Video Data. *arXiv preprint arXiv:2209.14792*, 2022. 1, 2, 7
- [44] Jascha Sohl-Dickstein, Eric A. Weiss, Niru Maheswaranathan, and Surya Ganguli. Deep Unsupervised Learning using Nonequilibrium Thermodynamics. In *ICML*, 2015. 1, 2
- [45] Jiaming Song, Chenlin Meng, and Stefano Ermon. Denoising Diffusion Implicit Models. In *ICLR*, 2021. 2
- [46] Yang Song and Stefano Ermon. Generative Modeling by Estimating Gradients of the Data Distribution. In *NeurIPS*, 2019. 1, 2
- [47] Thomas Unterthiner, Sjoerd van Steenkiste, Karol Kurach, Raphaël Marinier, Marcin Michalski, and Sylvain Gelly. FVD: A New Metric for Video Generation. In *ICLR Workshop*, 2019. 5
- [48] Ruben Villegas, Mohammad Babaeizadeh, Pieter-Jan Kindermans, Hernan Moraldo, Han Zhang, Mohammad Taghi Saffar, Santiago Castro, Julius Kunze, and Dumitru Erhan. Phenaki: Variable Length Video Generation from Open Domain Textual Description. In *ICLR*, 2023. 2
- [49] Vikram Voleti, Alexia Jolicoeur-Martineau, and Christopher Pal. MCVD-Masked Conditional Video Diffusion for Prediction, Generation, and Interpolation. In *NeurIPS*, 2022. 2
- [50] Fu-Yun Wang, Wenshuo Chen, Guanglu Song, Han-Jia Ye, Yu Liu, and Hongsheng Li. Gen-L-Video: Multi-Text to Long Video Generation via Temporal Co-Denoising. *arXiv preprint arXiv:2305.18264*, 2023. 2
- [51] Jiuniu Wang, Hangjie Yuan, Dayou Chen, Yingya Zhang, Xiang Wang, and Shiwei Zhang. ModelScope Text-to-Video Technical Report. *arXiv preprint arXiv:2308.06571*, 2023. 7
- [52] Wenjing Wang, Huan Yang, Zixi Tuo, HuiGuo He, Junchen Zhu, Jianlong Fu, and Jiaying Liu. VideoFactory: Swap Attention in Spatiotemporal Diffusions for Text-to-Video Generation. *arXiv preprint arXiv:2305.10874*, 2023. 5
- [53] Xiang Wang, Hangjie Yuan, Shiwei Zhang, Dayou Chen, Jiuniu Wang, Yingya Zhang, Yujun Shen, Deli Zhao, and Jin-gren Zhou. VideoComposer: Compositional Video Synthesis with Motion Controllability. In *NeurIPS*, 2023. 2, 6, 7
- [54] Chenfei Wu, Lun Huang, Qianxi Zhang, Binyang Li, Lei Ji, Fan Yang, Guillermo Sapiro, and Nan Duan. GODIVA: Generating Open-Domain Videos from Natural Descriptions. *arXiv preprint arXiv:2104.14806*, 2021. 5
- [55] Jay Zhangjie Wu, Yixiao Ge, Xintao Wang, Stan Weixian Lei, Yuchao Gu, Yufei Shi, Wynne Hsu, Ying Shan, Xiaohu Qie, and Mike Zheng Shou. Tune-A-Video: One-Shot Tuning of Image Diffusion Models for Text-to-Video Generation. In *ICCV*, 2023. 1, 2
- [56] Jun Xu, Tao Mei, Ting Yao, and Yong Rui. MSR-VTT: A Large Video Description Dataset for Bridging Video and Language. In *CVPR*, 2016. 5
- [57] Ting Yao, Yingwei Pan, Yehao Li, Chong-Wah Ngo, and Tao Mei. Wave-ViT: Unifying Wavelet and Transformers for Visual Representation Learning. In *ECCV*, 2022. 2
- [58] Ting Yao, Yehao Li, Yingwei Pan, Yu Wang, Xiao-Ping Zhang, and Tao Mei. Dual Vision Transformer. *IEEE Trans. on PAMI*, 2023. 2
- [59] Shengming Yin, Chenfei Wu, Jian Liang, Jie Shi, Houqiang Li, Gong Ming, and Nan Duan. Dragnuwa: Fine-grained Control in Video Generation by Integrating Text, Image, and Trajectory. *arXiv preprint arXiv:2308.08089*, 2023. 2

- [60] Shengming Yin, Chenfei Wu, Huan Yang, Jianfeng Wang, Xiaodong Wang, Minheng Ni, Zhengyuan Yang, Linjie Li, Shuguang Liu, Fan Yang, Jianlong Fu, Gong Ming, Lijuan Wang, Zicheng Liu, Houqiang Li, and Nan Duan. NUWA-XL: Diffusion over Diffusion for eXtremely Long Video Generation. *arXiv preprint arXiv:2303.12346*, 2023. [2](#)
- [61] Aohan Zeng, Xiao Liu, Zhengxiao Du, Zihan Wang, Hanyu Lai, Ming Ding, Zhuoyi Yang, Yifan Xu, Wendi Zheng, Xiao Xia, et al. GLM-130B: An Open Bilingual Pre-Trained Model. *arXiv preprint arXiv:2210.02414*, 2022. [3](#)
- [62] Lvmin Zhang, Anyi Rao, and Maneesh Agrawala. Adding Conditional Control to Text-to-Image Diffusion Models. In *ICCV*, 2023. [1](#), [2](#)
- [63] Daquan Zhou, Weimin Wang, Hanshu Yan, Weiwei Lv, Yizhe Zhu, and Jiashi Feng. Magicvideo: Efficient Video Generation with Latent Diffusion Models. *arXiv preprint arXiv:2211.11018*, 2022. [7](#)